Crushing performances of Kirigami modified honeycomb structure in three axial directions

Zhejian Li[1], Qiusong Yang[2], Rui Fang[2], Wensu Chen[1]*, Hong Hao[1]*

[1] *Centre for Infrastructural Monitoring and Protection*
School of Civil and Mechanical Engineering, Curtin University, Australia
[2] *School of Civil Engineering, Guangzhou University, China*

*corresponding author: wensu.chen@curtin.edu.au; hong.hao@curtin.edu.au

Abstract

A novel Kirigami (cut and fold) modified honeycomb structure is proposed in this study, aiming to reduce the initial peak force under out-of-plane crushing while maintaining the high energy absorption capacity, as well as increasing the in-plane crushing resistance. Three aluminium hexagonal honeycomb structures: standard honeycomb (HC), sheet reinforced honeycomb (RHC), and Kirigami modified honeycomb (KHC) structures are prepared and tested under quasi-static compression in three axial directions. The compressive properties of the proposed Kirigami modified honeycomb are compared with standard honeycomb and reinforced honeycomb in three axial directions. Numerical method is employed to adjust the wall thickness of HC so that its relative density is the same as RHC and KHC for fair comparisons on the crushing performances. Numerical model of standard honeycomb (HC) is calibrated and updated with the adjusted wall thickness to compare with the test results of reinforced and Kirigami modified honeycomb structures of the same relative density. The KHC demonstrated significant improvement on energy absorption capability as compared to the other two honeycombs in all three axial directions. Under out-of-plane crushing, KHC does not develop an initial peak force, while its average crushing resistance remains at a similar level as RHC, and is 17.6% higher than that of HC. Under the in-plane 1 compression, the average crushing resistance of KHC is around 5.2 and 7.5 times of that of HC and RHC, with an even lower uniformity ratio. The KHC shows a moderate improvement in crushing resistance in in-plane 2 direction, compared with the other two honeycombs. These results demonstrate the significant improvement of Kirigami modification on the crushing performance of honeycomb structures.

Keywords: Kirigami modified honeycomb; Energy absorption; Quasi-static compression; Three axial directions

1 Introduction

As one of the most representative cores of sandwich structures, hexagonal honeycomb structures have been widely used in various engineering fields including structural [1], aviation [2, 3], automobile [4], railway vehicles [5] and aerospace [6] industries. Over the past decades, extensive research on the compressive responses of honeycomb structures along both the out-of-plane and in-plane axes had been carried out for numerous loading scenarios. Wierzbicki and Abramwicz investigated the axial crushing mechanics and collapsing modes of the thin-walled metal honeycomb structures [6-8]. Cote et al [9] and Radford et al [10] studied the dynamic crushing response of square honeycomb structures. Kumar et al [11], Zhu et al [12] and Nurick et al [13] experimentally examined the structural response of square and hexagonal honeycomb panels under high-intensity blast loads. Sun et al [14], Xu et al [15] and Wang et al [16] studied the effect of loading rates on out-of-plane mechanical responses of hexagonal honeycomb structures. Studies on the in-plane crushing responses of the hexagonal honeycomb structures and the effect of loading rates were carried out by Gibson and Ashby [17] as well as Hu and Yu [18].

Under out-of-plane quasi-static compression, honeycomb structure undergoes a short elastic linear deformation with a drastic rise in crushing force, followed by a sudden reduction of crushing resistance and a long plateau stage with uniform crushing resistance which is an ideal feature for energy absorption, until the densification of the structure [6, 19]. However, the high initial peak force of honeycomb structures under out-of-plane crushing is non-ideal for energy absorption and structural protection. Furthermore, with the increase of crushing speed, the initial peak crushing resistance of honeycomb structures in the out-of-plane direction could increase several times while the average crushing resistance is less affected [14, 15]. These two characteristics of honeycomb structures under out-of-plane compressive loads, i.e., high initial peak force and strong loading rate dependency of the initial peak, are not ideal for energy absorbing applications [20, 21]. Although the initial peak force is not presented in honeycomb under in-plane compression, its resistances along in-plane directions are considerably lower compared to that of out-of-plane direction.

Depending on the cell size and manufacturing methods, some modifications have been proposed to increase the energy absorption capacity or improve the crushing characteristics of honeycomb structure for energy absorption applications. Two common methods for fabricating metal sheet honeycomb structures are expansion and corrugation manufacturing process [22, 23], as shown in Figure 1 (a, b). For the expansion manufacturing of honeycomb, the undeformed flat metal sheets are stacked and strip bonded to form a “honeycomb before expansion” or HOBE block. The block is then stretched along the in-plane direction and the stacked sheets are deformed at the bonded strips to form the hexagonal honeycomb structure. This method requires high bonding strength and the wall thickness of the cell is limited, as the layers in HOBE block required to remain bonded during stretching. Thus, the expansion manufactured honeycomb structures often have low relative density, small cell size and thin cell wall [22]. To enhance the energy absorption characteristics of the expansion manufactured honeycomb, it can be combined with other structures such as tube reinforced honeycomb structures [24-27] or used as a filler [5, 28-30] similar to foam-filled structures. Different to the expansion manufacturing process, the metal sheets are firstly corrugated using a press, they are stacked and then either adhesively bonded or welded during the corrugation manufacturing process. As a press is used to from the corrugation layers of honeycomb, larger unit cells, higher relative density and thicker cell wall of the honeycomb structures can be achieved for corrugation manufacturing process [22]. Therefore, the modifications on corrugated structures, such as the addition of foam fillers [31-34], sheet reinforced [23, 35, 36], graded layers [37, 38], hierarchical cell wall [39-41] and origami honeycomb [42, 43] etc., could be implemented here on corrugation manufactured honeycomb structures in order to enhance the energy absorption characteristics.

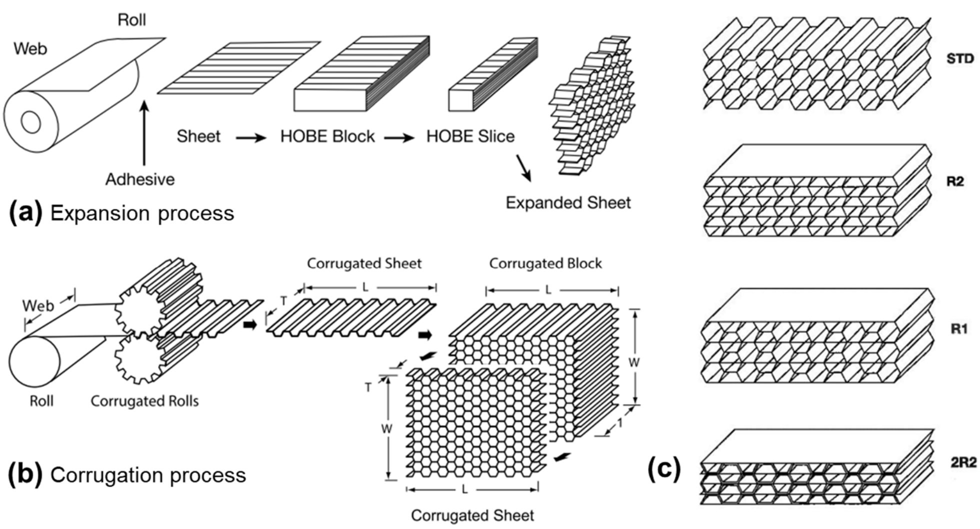

Figure 1. Two common manufacturing process of honeycomb; (a) Expansion process; (b) Corrugation process [23]; (c) Commercially available standard and reinforced hexagonal honeycomb structures made from corrugation process [36]

Many of the modifications on corrugation-manufactured honeycomb structures have some drawbacks. Foam fillers significantly increase the energy absorption, but they also increase the mass of the light-weight honeycomb. Foam fillers can be expensive to machine and to bond with the structure [31]. Layer density graded honeycomb structures may be effective for dynamic crushing under a certain range of crushing speeds and in the graded orientation only. Hierarchical honeycombs have complex geometry and can be difficult to fabricate, especially in large size. Sheet reinforced hexagonal honeycomb is one of the few, if not the only commercially available modified honeycomb structure with enhanced energy absorption capacity [44], as shown in Figure 1 (c). However, until now there are limited research on the mechanical properties of such sheet reinforced honeycomb structures. No comparative study between the standard and sheet reinforced honeycomb structures of the same density has been reported yet. The investigation on the in-plane mechanical properties of the sheet reinforced honeycomb is also deficient.

Based on the Kirigami modification on single layer trapezoidal corrugated unit [45], a relatively inexpensive and simple Kirigami modification is proposed for the corrugation fabricated honeycomb structures in this study. The corrugated layers are firstly laser cut and folded along the designed creases and then adhesively bonded to other layers, the same as in the corrugation manufacturing process of a honeycomb structure. However, interlayers between corrugated sheets similar to reinforced honeycomb are required for this modification to provide support to the fold-ins on in-plane directions. The proposed Kirigami modification changes the 2D reinforced honeycomb into a 3D structure and significantly increase the in-plane crushing resistances while reducing the initial peak force under out-of-plane compression. In this paper, three honeycomb structures, including standard hexagonal honeycomb (HC), reinforced honeycomb (RHC) and Kirigami modified honeycomb (KHC), are compared for their quasi-static crushing resistance and energy absorption capacity in three axial directions. The quasi-static compressive tests were carried out in three axial directions for three blocks of aluminium honeycomb structures. Due to the availability of the aluminium sheet, the relative density of standard honeycomb (HC) was slightly lower than those of the other two (RHC, KHC). To fairly compare these structures, a numerical model of the standard honeycomb (HC) was firstly constructed and validated with test data. The wall thickness of the standard honeycomb (HC) was then adjusted to have the same relative density as the other two honeycomb specimens (RHC, KHC). Load-displacement curves, peak and average crushing resistance, and energy absorption were used as criteria for comparing the quasi-static compressive properties of three honeycomb structures in three axial directions.

2 Quasi-static compression set-up

2.1 Specimen preparation

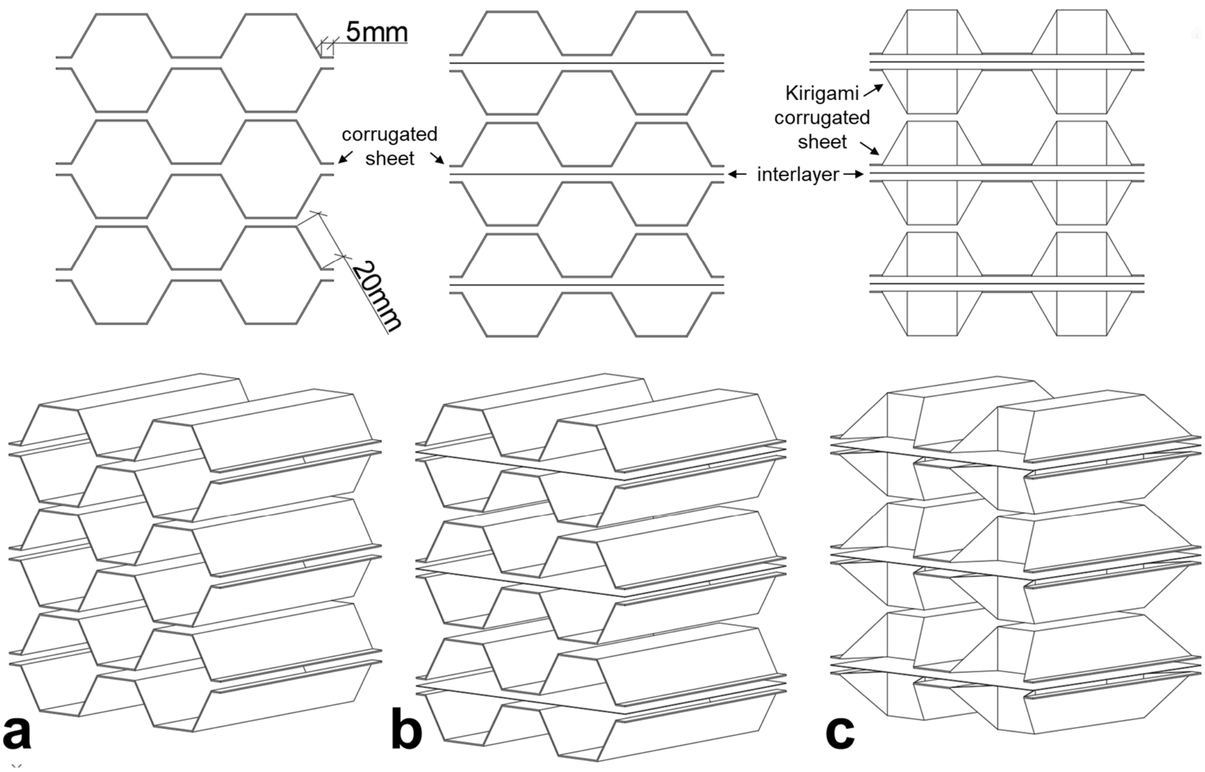

Figure 2. Schematic drawings of (a) standard honeycomb (HC); (b) sheet reinforced honeycomb (RHC); (c) Kirigami modified honeycomb (KHC)

Three types of honeycomb structures including standard honeycomb, sheet reinforced honeycomb and Kirigami modified honeycomb are considered, as shown in Figure 2. The standard honeycomb structure is abbreviated as HC, sheet reinforced honeycomb and Kirigami modified honeycomb are noted as RHC and KHC, respectively. The hexagons on all honeycomb structures have the same side length of 20 mm, with a 5 mm flat strip on each side of the corrugating sheet for bonding. All three types of honeycomb specimens were prepared with the corrugation process, where the layers were firstly corrugated and then bonded. There were six corrugated sheets for each specimen, where three flat sheet interlayers were used to separate the corrugated sheets for RHC and KHC.

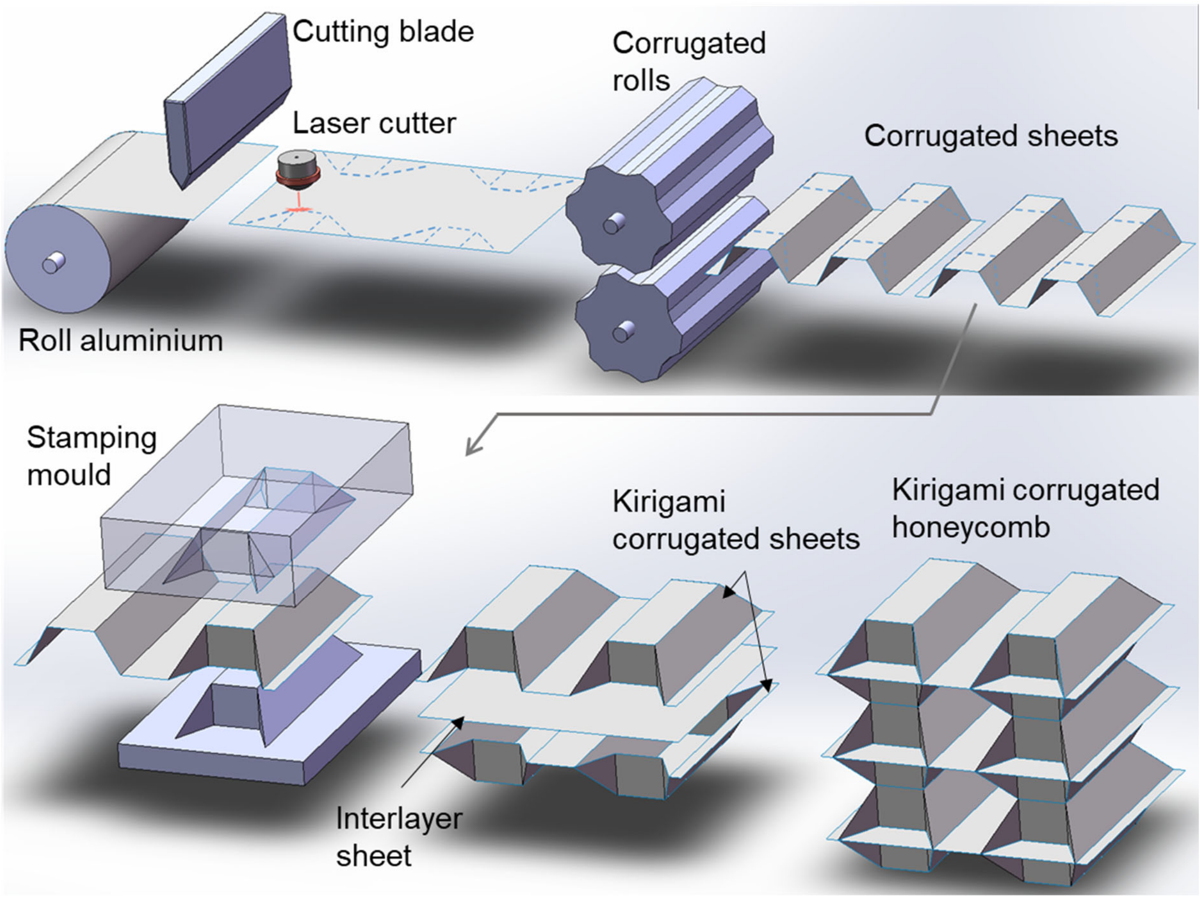

Figure 3. Illustrative manufacturing process for KHC

For KHC, a manufacturing process similar to corrugation process of honeycomb shown in Figure 1 (b), is proposed for potential mass production. As shown in Figure 3, two more steps are required for KHC: laser cutting of the fold-in pattern and partial stamping of the fold-ins, both can be achieved relative easily compared to some current modifications such as 3D-printed hierarchical wall. In this study, the aluminium sheet material was laser cut first to make the folding process easier. A 3D-printed mould shown in Figure 4, was then used for folding the Kirigami corrugated sheets. Each corrugated layer was also folded according to the specific design before bonding. Bonding glue ergo 1655 NB was applied between the contacted horizontal flat areas between the sheets. All three honeycombs, HC, RHC and KHC have the same overall dimensions of 110×105×100 mm as marked out in Figure 5.

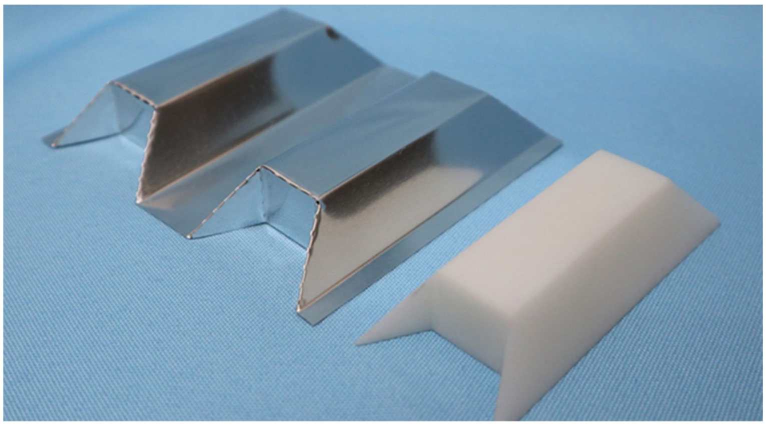

Figure 4. A folded layer of Kirigami corrugate sheet and 3D printed mould used for folding

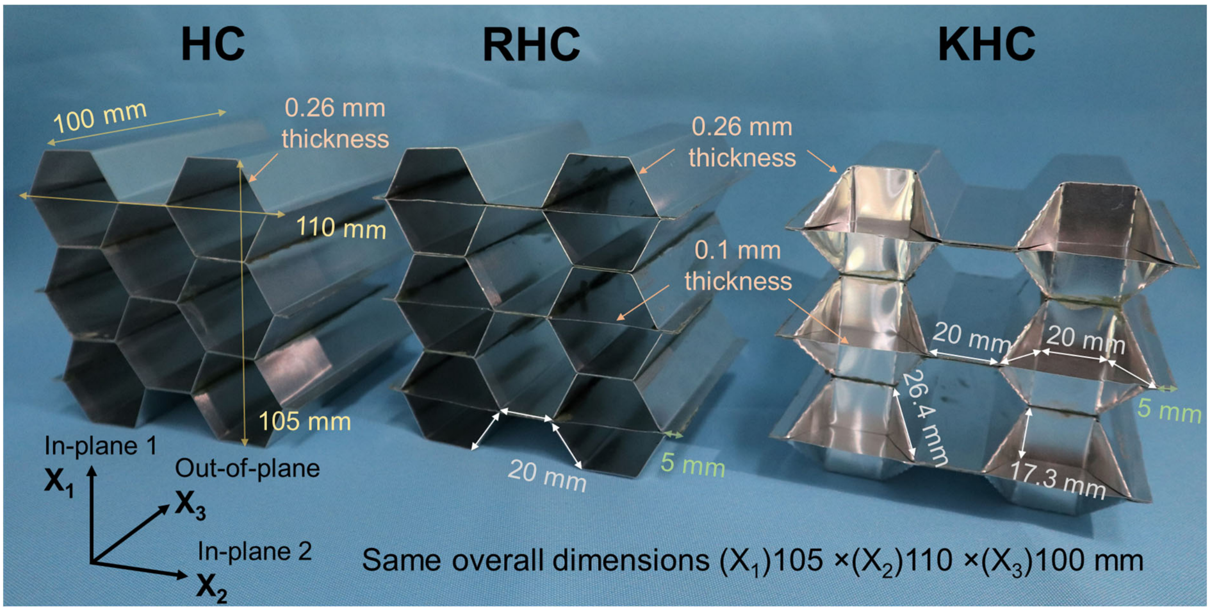

Figure 5. Specimens of standard honeycomb (HC), reinforced honeycomb (RHC) and Kirigami modified honeycomb (KHC) prepared with corrugation process (left to right)

For Kirigami modified honeycomb, a portion of the top horizontal unit cell of the corrugate sheet is folded by 90° as shown in Figure 6. Three adjacent faces become perpendicular to the horizontal plane after folding. Dash lines along the designed creases were laser cut to enhance the quality and reduce the difficulty of the folding process. The creases were laser cut at 1 mm in length for every 4 mm, with a width of 0.1 mm. This creased dash line configuration was selected after testing dozens of laser-cutting configurations [45]. The geometric parameters of the Kirigami modification are dependent on the side length, *a*, for the hexagonal honeycomb where six sides of the cell have the same length. Other parameters can be expressed as follows:

$$b = h = \frac{\sqrt{3}}{2} \cdot a = 17.3mm \quad (1)$$

$$c = \sqrt{a^2 + h^2} = \frac{\sqrt{5}}{2} \cdot a = 26.5mm \quad (2)$$

$$\alpha = \arctan(b / a) = 40.9° \quad (3)$$

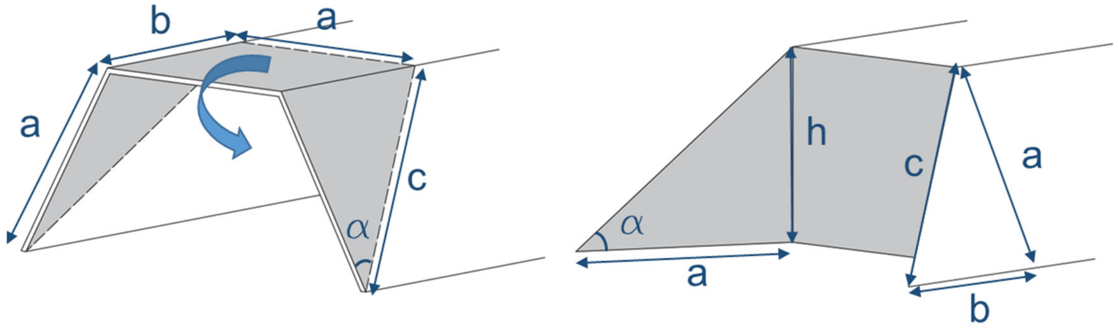

Figure 6. Kirigami modification on a unit cell of a corrugation sheet for hexagonal honeycomb

All specimens were made from Aluminium 1060 where the corrugated sheet has a thickness of 0.26 mm, and the interlayers on RHC and KHC had a thickness of 0.1 mm. The mechanical properties of Al 1060 were tested previously [45] according to ASTM-E8M [46] and they are listed as follows, yield strength: 110MPa, Young's modulus: 70 GPa and density: 2700 kg/m^3, the true stress-strain curve of Al 1060 is shown in Figure 7. Due to the additional interlayers within the RHC and KHC, the relative densities or volumetric densities of RHC and KHC specimens are slightly higher than that of HC. The relative density for HC is 2.0% and the relative densities for RHC and KHC are 2.3%. The aluminium mass of HC specimen is 63g, and the mass of RHC and KHC are 72g.

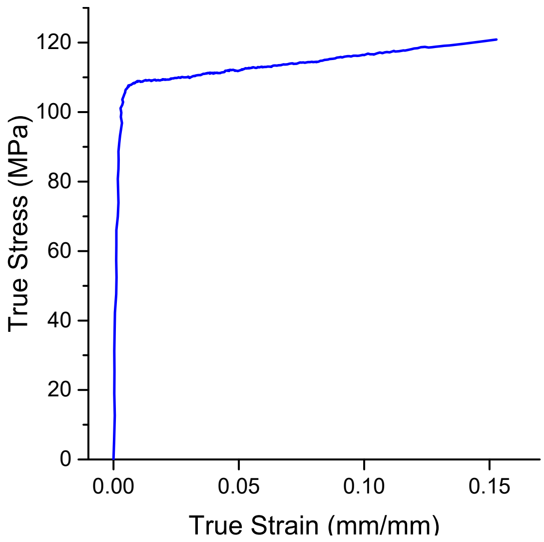

Figure 7. True stress-strain curve of aluminium 1060 sheet

2.2 Test set-up

Crushing tests were carried out in three axial directions for the three honeycomb specimens under quasi-static loading condition. SUNS® CMT5504 testing machine with a loading capacity of 50 kN was used for the compressive tests. The honeycomb specimens were simply placed between the crushing head and the support plates without constraint. Circular crushing and supporting discs with a diameter of 150 mm were used for out-of-plane compression and square plates with a side length of 200 mm were used for in-plane compression. To ensure the quasi-static crushing loading condition, constant crushing speed of 5 mm/min [47] was applied for all tests until the strain reached approximate 0.85. Two specimens were tested for each honeycomb in each loading direction. However, a third repetitive test was carried out for the cases when the first two test results have relatively large discrepancy.

3 Test results and discussion

3.1 Out-of-plane compression

Out-of-plane compressive properties of the honeycomb structures are crucial for energy absorption and load-bearing applications. The load-displacement curves of the three honeycomb structures under out-of-plane compression are shown in Figure 8. Initial peak, average crushing force, uniformity ratio and energy absorption for individual tests are listed in Table 1. The initial peak force is defined as the peak crushing force at the initial stage of crushing, where the initial stage is defined by the strain less than 0.1 in this study. The average crushing force is the average of the crushing force until the densification of the structure, where a sudden increase in crushing resistance occurs. The ratio between the initial peak and average crushing force is named as uniformity ratio (*U*), which is used as an important parameter to evaluate the energy absorption performance of the structure. The energy absorption is measured by the integrating the load-displacement curves from beginning to the densification of the structure. It should be noted that the initial peak force may be in low value and could be even lower than the average crushing force, due to the easy deformation initiation of the structure. For instance, KHC test 02 shows a lower initial peak than the average crushing force under out-of-plane crushing as shown in Figure 8 (c). The uniformity ratio, *U*, for such case, is set to be 1 as shown in Table 1.

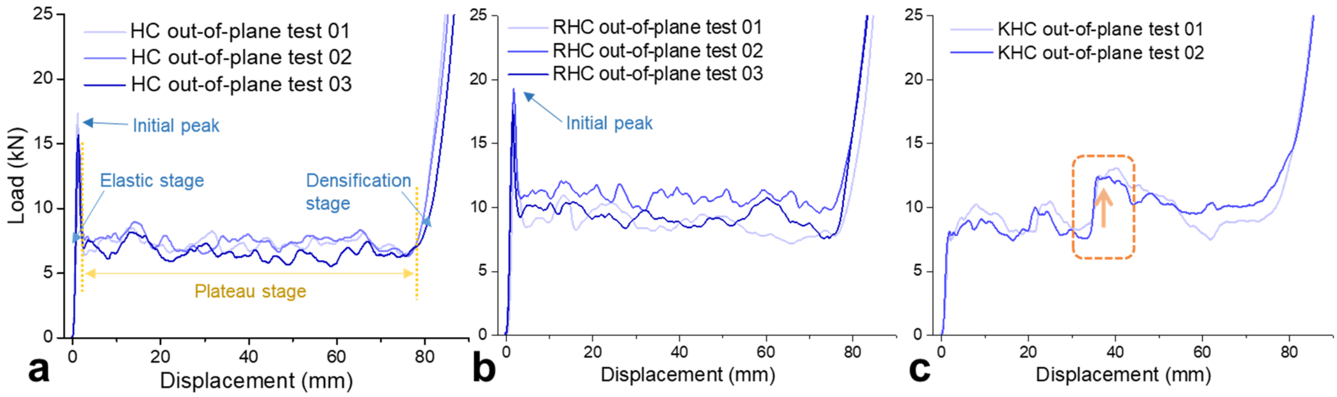

Figure 8. Load-displacement curves of (a) HC; (b) RHC; (c) KHC under out-of-plane compression

As shown in Figure 8, sheet reinforced honeycomb (RHC) demonstrates similar out-of-plane crushing response as HC but with higher peak crushing and average resistance force, where a sharp rise and drop of crushing force at the initial stage followed by a long plateau stage with slight fluctuations. KHC structure shows no sudden sharp rises and drops in crushing force at the initial stage. However, as shown in Figure 8 (c), a moderate rise in crushing resistance as circled can be observed at middle deformation around 35 mm of displacement. Compared to the standard honeycomb (HC), RHC structures exhibit an enhanced energy absorption capacity. By introducing additional thin sheets between layers, RHC structures show a noticeable increase in average crushing resistance and a slight increase in initial peak, resulting in a slight reduction of uniformity ratio as compared to HC structures. Further improvements are also observed by Kirigami modification on RHC structures. As shown, the initial sudden rise and drop in crushing resistance observed in HC and RHC are eliminated with Kirigami modification. Under out-of-plane crushing, the KHC structure has demonstrated a more uniform crushing resistance throughout the compression, while its average crushing resistance remained at a similar level as RHC structure.

Table 1. Initial peak, average crushing force, uniformity ratio and energy absorption of three honeycombs under out-of-plane compression

Out-of-plane	**test number**	**P_{peak} (kN)**	**P_{ave} (kN)**	**$U=P_{peak}/P_{ave}$**	**EA (J)**
HC	01	17.34	7.32	2.37	572.12
	02	15.15	7.49	2.02	584.95
	03	15.66	6.68	2.34	527.00
	Average	**16.05**	**7.16**	**2.24**	**561.36**
RHC	01	17.23	8.78	1.96	673.88
	02	19.31	10.85	1.78	820.12
	03	17.62	9.28	1.90	710.36
	Average	**18.05**	**9.64**	**1.88**	**734.79**
KHC	01	10.25	9.47	1.08	731.46
	02	9.10	9.48	1.00	711.23
	Average	**9.68**	**9.48**	**1.04**	**721.35**

Both HC and RHC show similar deformation throughout the crushing. Typical multiple folds are observed near the contacts and wall buckling is shown away from the contacting interfaces, as shown in Figure 9 (a, b) at 10 and 35 mm displacement. KHC deforms differently to the other two honeycombs at the early stage. With the Kirigami modifications at two ends circled in Figure 9 (c), the compressive strength is significantly reduced at the initial stage, as some portions of the vertical walls are folded parallel to the crushing surface, and provide little support at initial stage under out-of-plane crushing. The middle section of KHC is less deformed than HC and RHC at 10 mm displacement. Under further compression, the remaining middle sections on KHC are in contact with the crushing and supporting plates and the deformation on these middle sections initiated. As shown in Figure 9 (c) at around 35 mm displacement, the circled fold-ins of KHC are completely crushed and middle sections start to deform, leading to a noticeable increase in crushing resistance at 35 mm of displacement in Figure 8 (c).

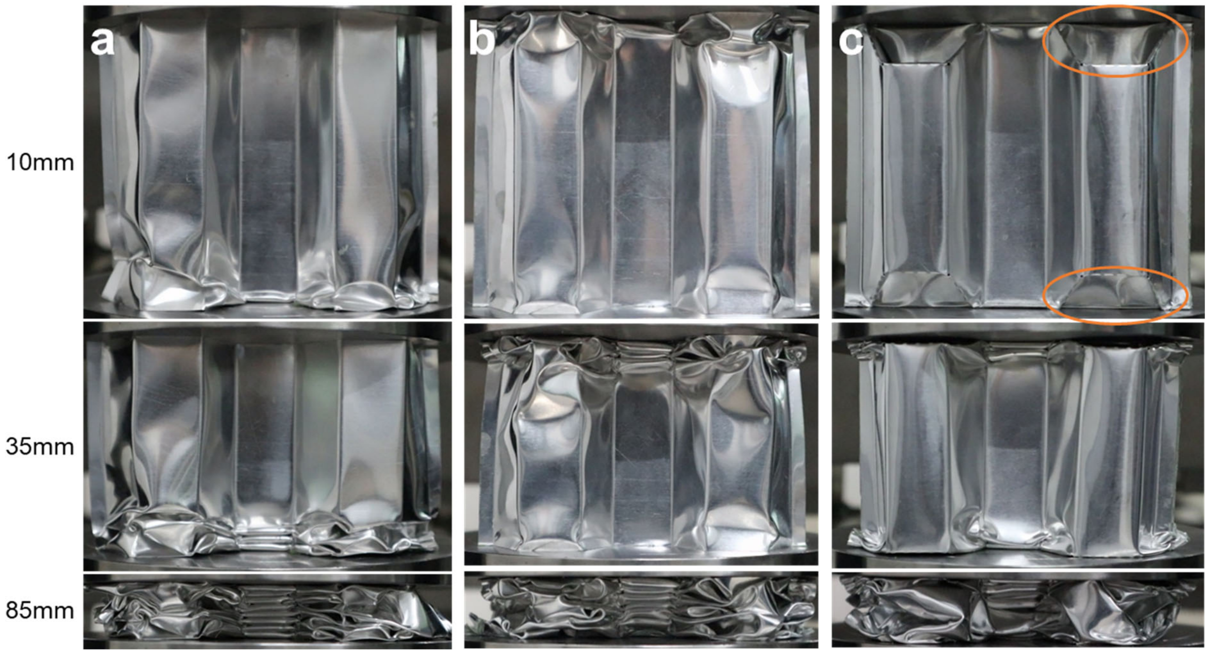

Figure 9. Deformation comparisons of (a) HC; (b) RHC; (c) KHC at 10, 35 and 85 mm displacement (from top to bottom) under out-of-plane quasi-static compression

3.2 In-plane compression

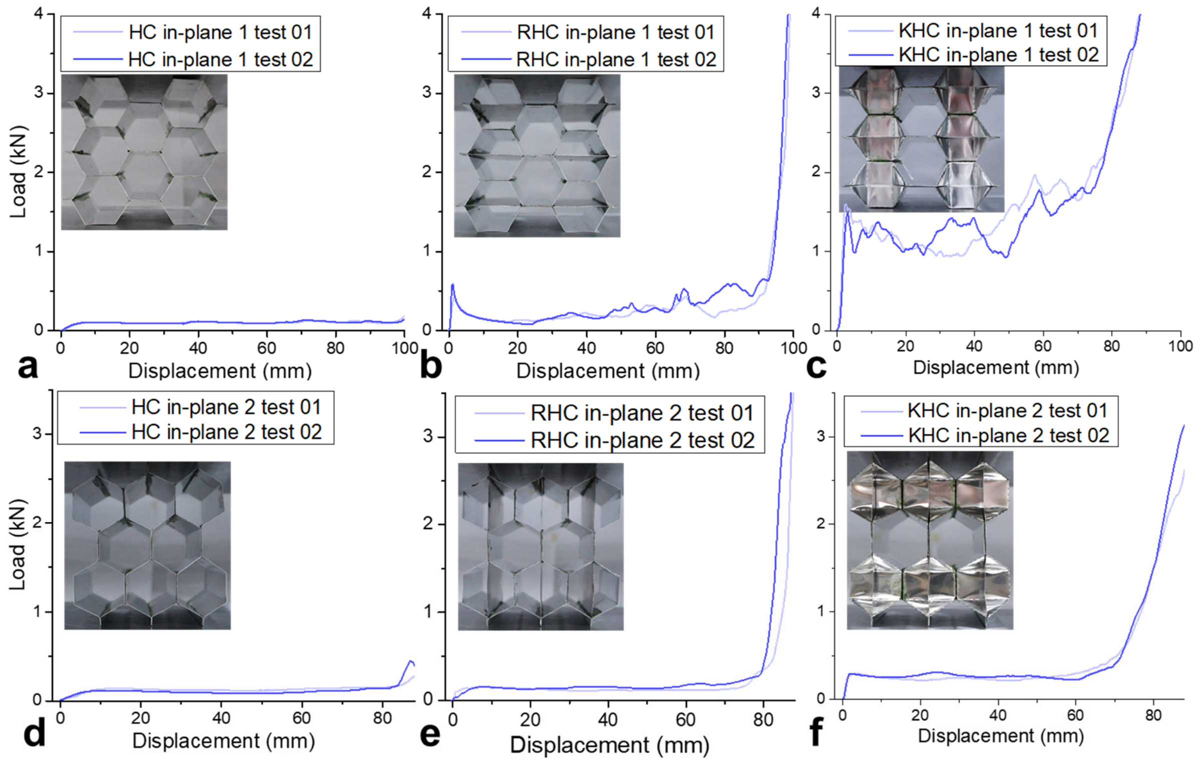

Figure 10. Load-displacement curves of (a) HC; (b) RHC; (c) KHC under in-plane 1 compression; Load-displacement curves of (d) HC; (e) RHC; (f) KHC under in-plane 2 compression

The load-displacement curves of three honeycomb structures under both in-plane directions are shown in Figure 10. Key parameters of the compressive properties under in-plane 1 and 2 directions are listed in Table 2 and Table 3, respectively. Very different crushing responses are observed for three honeycombs under in-plane 1 compression. The crushing resistance of HC under in-plane 1 compression is very low, with an average resistance of 100 N, which is about 1.3% compared to its out-of-plane crushing resistance. However, the crushing process of HC seems uniform with no high initial peak force. With the interlayer sheet, the average crushing resistance of RHC under in-plane 1 compression is more than twice than that of HC. Furthermore, a distinct initial peak is shown for RHC under in-plane 1 compression, resulting in the highest uniformity ratio of RHC among the three honeycombs. Gradual increase in crushing resistance can also be observed at the later stage for RHC. KHC shows superior energy absorption performance under in-plane 1 compression out of these three honeycombs. The average crushing resistance as well as the energy absorption are significantly improved, around 12 times higher than that of HC and around 5 times higher than RHC. The initial peak force of KHC is also relatively low. Its uniformity ratio under in-plane 1 crushing remained in a similar level as HC at around 1.2, indicating great energy absorption capacity.

Table 2. Initial peak, average crushing force and uniformity ratio of three honeycombs under in-plane 1 compression

In-plane 1	**test number**	**P_{peak} (N)**	**P_{ave} (N)**	**$U=P_{peak}/P_{ave}$**	**EA (J)**
HC	01	106	99	1.07	9.63
	02	107	101	1.06	10.02
	Average	**107**	**100**	**1.07**	**9.83**
RHC	01	442	224	1.97	20.50
	02	591	280	2.11	25.96
	Average	**517**	**252**	**2.05**	**23.23**
KHC	01	1611	1318	1.22	94.13
	02	1483	1280	1.16	94.55
	Average	**1547**	**1299**	**1.19**	**94.34**

HC has similar crushing responses under in-plane 2 compression and in-plane 1 compression due to the symmetry of the HC. However, slight increases in both initial peak and average crushing resistance are shown for in-plane 2 compression, which is caused by the stress-free edges under in-plane 1 compression [45]. RHC shows the similar crushing response as HC under in-plane 2 compression, with a higher average crushing resistance at around 150 N. The addition of interlayer in RHC is less effective in terms of crushing resistance under in-plane 2 compression than that of in-plane 1 compression. KHC shows a higher crushing resistance than that of HC and RHC, but the increment is not as large as that along in-plane 1 direction. Initial peak force for all three honeycombs under in-plane 2 compression is very low. It should be noted that the load-displacement curves of KHC started to rise significantly at around 70 mm of displacement where the 'densification' is reached. However, the actual structure densification of KHC is not yet reached at 70 mm of displacement, further crushing can be carried out. Due to its unique geometry, KHC reached the second state of deformation at 70 mm displacement, where a much higher crushing resistance occurs. Details of this second stage are discussed in deformation analysis of the three structures. For consistency, the 'densification' of KHC is considered reached at 70 mm displacement as it is the starting point of the sudden increase in crushing resistance. 70 mm is used to calculate the average crushing resistance of KHC in Table 3.

Table 3. Initial peak, average crushing force and uniformity ratio of three honeycombs under in-plane 2 compression

In-plane 2	**test number**	**P_{peak} (N)**	**P_{ave} (N)**	**$U=P_{peak}/P_{ave}$**	**EA (J)**
HC	01	137	126	1.09	10.74
	02	117	104	1.13	8.71
	Average	**127**	**115**	**1.10**	**9.72**
RHC	01	156	141	1.11	11.58
	02	155	156	1.00	12.38
	Average	**156**	**149**	**1.05**	**11.98**
KHC	01	272	260	1.05	18.26
	02	292	272	1.07	19.41
	Average	**282**	**266**	**1.06**	**18.84**

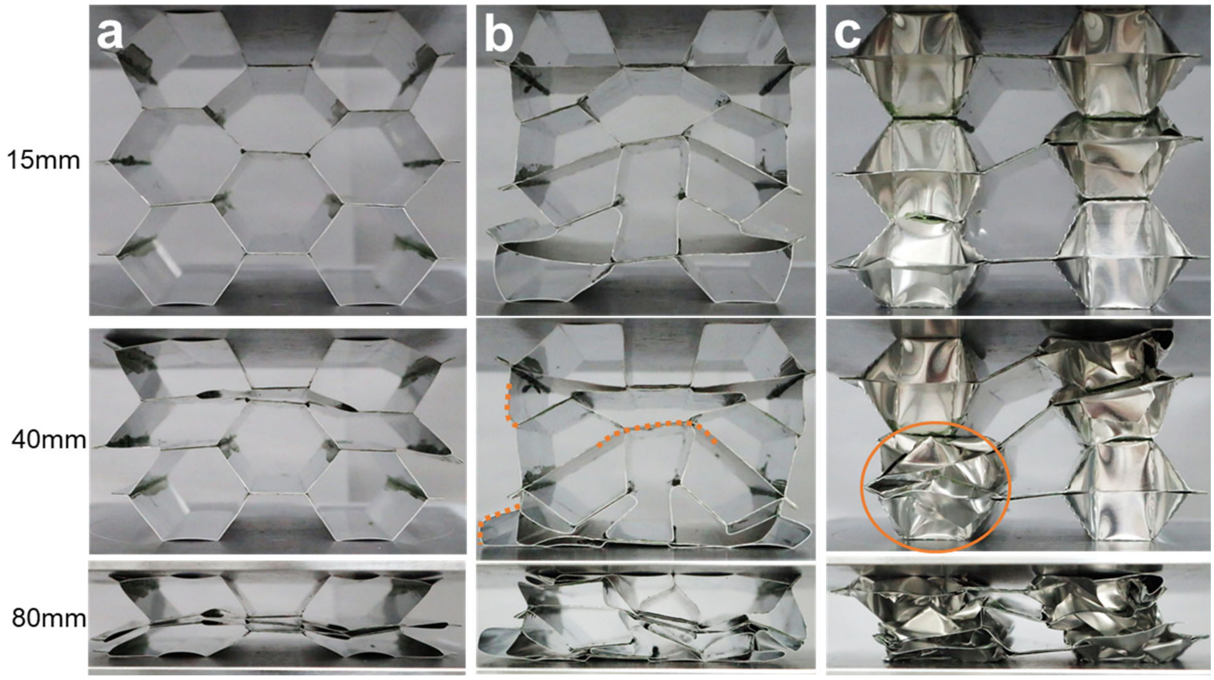

Figure 11. Deformation comparisons of (a) HC; (b) RHC; (c) KHC at 15, 40 and 80 mm displacement (from top to bottom) under in-plane 1 quasi-static compression

Deformations of three honeycombs at 15, 40 and 80 mm displacement under in-plane 1 crushing are shown in Figure 11. Under in-plane 1 crushing, HC expands outwards and 2D bending deformations appear only near the existing plastic hinge lines introduced during the corrugation process. The cell walls between the static plastic hinge lines experience minimal deformation. Thus, the crushing resistance of HC remains uniform and at a very low value under in-plane 1 crushing. For RHC, the corrugated layers cannot expand outwards due to the additional interlayer bonds the corrugated sheets. These interlayers constrain the initial deformation of RHC and maintain its shape at the initial contact, resulting in a peak force at initial stage. As shown in Figure 11 (b), the width of RHC is noticeably smaller than that of HC structure. Furthermore, due to the restriction on the horizontal expansion of RHC, some parts of the cell walls between the plastic hinge lines as well as the interlayer start deforming as marked in Figure 11 (b), leading to doubling of the crushing resistance compared to HC under in-plane 1 compression. However, most of the deformation of RHC is still in 2D bending mode and the crushing resistance along in-plane 1 direction is low. KHC shows completely different deformation mode from the other two honeycombs. With the Kirigami modification, some portions of the cell walls become vertical, and these are also connected to the remaining of the cell walls. After the Kirigami modification, the deformation mode changes from 2D bending that mostly concentrated near folding lines to 3D buckling of entire fold-ins, and leads to around 5 times increase in crushing force as compared to RHC. It should be noted that the interlayer and sidewalls of KHC experience less deformation compared to its fold-ins.

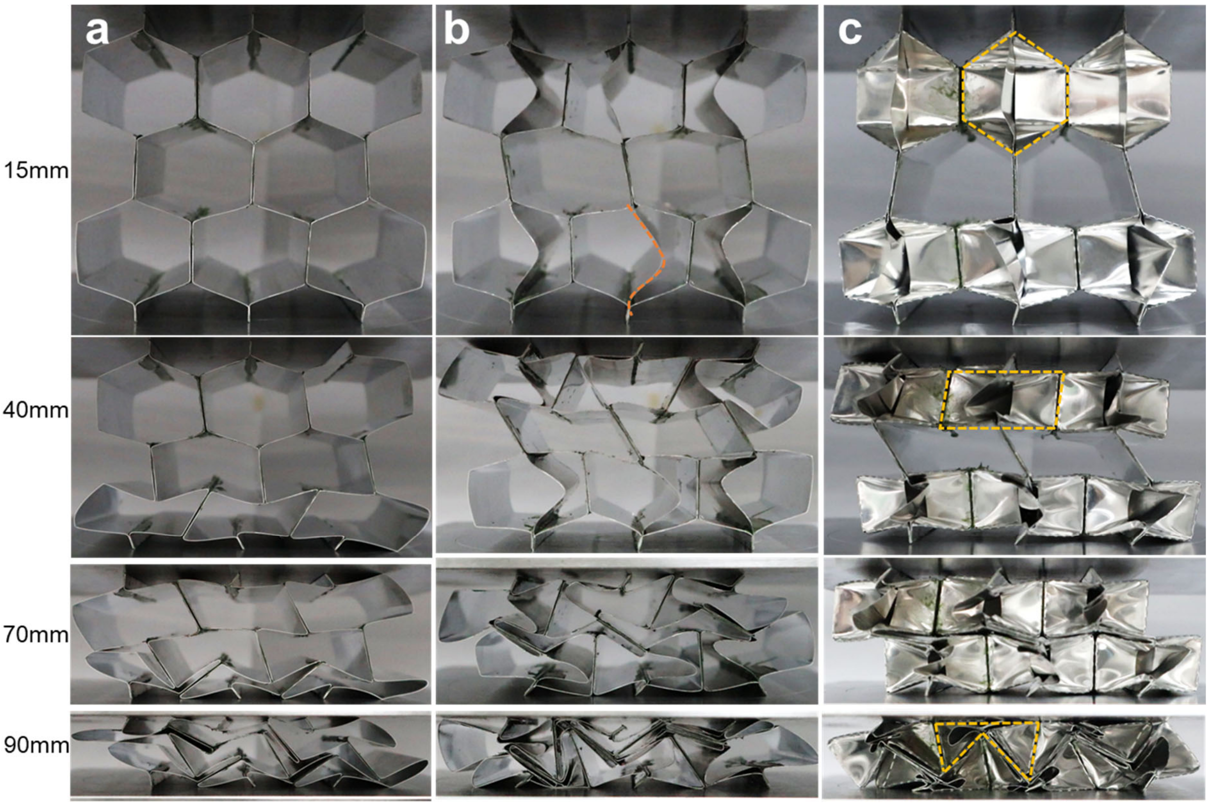

Figure 12. Deformation comparisons of (a) HC; (b) RHC; (c) KHC at 15, 40, 70 and 90 mm displacement (from top to bottom) under in-plane 2 quasi-static compression

Out of three axial directions, the crushing resistance under in-plane 2 direction of all three honeycombs are the most similar and their average crushing resistance are all below 300 N, and the uniformity ratios are very low. As shown in Figure 12, the deformations of HC and RHC are similar under in-plane 2 crushing, except that for RHC the additional bending of the bonded interlayer can be observed as marked in the figure. The fold-ins on KHC provide little support under in-plane 2 compression, the hexagonal unit cells deform and become rectangle in shape, similar to the other two honeycombs. However, at displacement around 70 mm, the two rows of deformed unit cells are in contact, and the fold-ins start to buckle. These 3D buckling of the fold-in faces cause a sharp rise in crushing resistance, as shown in Figure 10 (f) at around 70 mm, and it could be mistakenly recognized as the 'densification' of the KHC structure. In reality, the second stage of deformation with much higher crushing resistance is reached for KHC, while the fold-ins are in contact and start to buckle, and the true densification of the structure is not yet reached. It should be noted that the 2nd stage of KHC crushing (after 70 mm) is not included for calculating the average crushing resistance along in-plane 2 direction, due to the significant differences in crushing resistances between 1st and 2nd stage of deformation.

4 Numerical simulation

4.1 Numerical modelling

As previously mentioned, the three honeycomb specimens used for testing are of different relative density due to the additional interlayers in RHC and KHC structures. HC has a relative density of 2.0%, slightly lower than that of RHC and KHC, which both have relative densities of 2.3%. To fairly compare the compressive properties of three honeycombs, numerical model of HC is firstly constructed in LS-DYNA, and validated with test data. The wall thickness of the validated HC model is then adjusted so that HC would have the same relative density as the other two honeycombs. Their compressive properties in three axial directions are then compared.

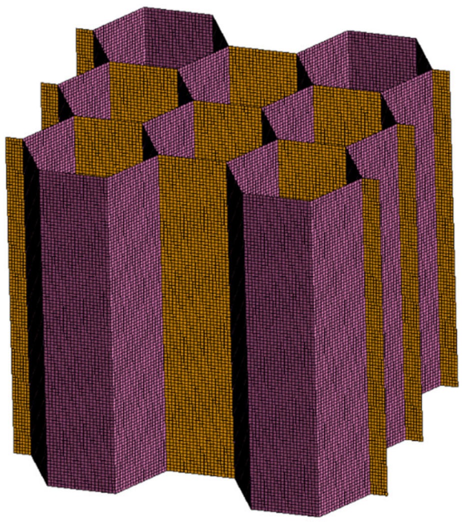

Figure 13. Numerical model of standard honeycomb (HC)

LS-DYNA is used for numerical modelling of the HC structure in this study. Shell element with mesh size of 1 mm is used after performing the mesh convergence test. As shown in Figure 13, the sections of HC are divided into orange and purple colours and are assigned with different thicknesses of 0.52 mm and 0.26 mm, matching the thicknesses of the HC specimen tested in the study, where the glue thickness is not considered. An elasto-plastic material model, *MAT_24 PIECEWISE LINEAR PLASTICITY, is used to model the 1060 aluminium sheet. Material properties and stress-strain data of Al 1060 shown in section 2.1 are applied in the material model. The friction coefficient of 0.25 [48] is used in this study. Both supporting and crushing plates are modelled as rigid solid.

4.2 Model validation

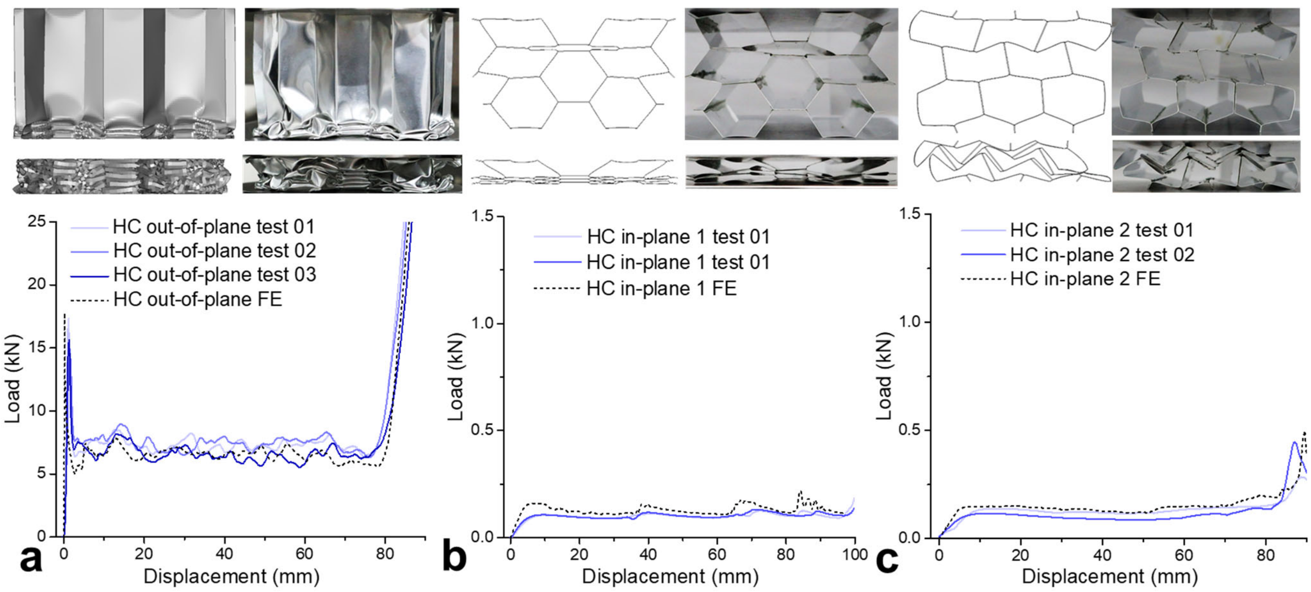

Figure 14. Load-displacement curves and deformation comparisons at 35 mm / 84 mm for HC under (a) out-of-plane; (b) in-plane 1; (c) in-plane 2 compression

Comparisons of three axial compressive response from FE and test results for HC with the corrugating sheet thickness of 0.26 mm are shown in Figure 14. The initial peak and average crushing resistances are compared and listed in Table 4. It is observed that the FE results slightly overestimate the initial peak force of HC under crushing in three axial directions. As imperfections introduced in specimen manufacturing are not included in the FE models, the average crushing force obtained from FE simulation slightly underestimates out-of-plane compression, and overestimates both in-plane compressions. The presence of glue used in the testing specimens could also affect the crushing resistance, as it slightly increases the wall thickness hence a higher buckling resistance under out-of-plane compression. For in-plane compression, the bending deformations mostly concentrate along crease lines, instead of the glued surfaces. Therefore, the FE models without considering imperfections show a slightly higher crushing resistance in both in-plane directions. Nevertheless, the overall trends of load-displacement curves and deformation patterns of the FE simulation results agree well with the test results for HC under compression in all three directions. The uniformity ratio of HC from tests and FE are 1.06 and 1.23, respectively for in-plane 1 compression, 1.10 and 1.09 for in-plane 2 compression. Overall, the FE model is considered yielding reasonable predictions of crushing responses of HC and is therefore used in the investigation of responses of HC with increased wall thickness.

Table 4. Average crushing resistance and energy absorption comparison between FE and test for HC under three axial quais-static compression

	P_{ave}			**EA**		
	Test	FE	Error	Test	FE	Error
Out-of-plane	7.16 kN	6.56 kN	-8.4%	561.36 J	532.46 J	-5.1%
In-plane 1	100 N	128 N	28%	9.82 J	12.55 J	27.8%
In-plane 2	115 N	137N	19.1%	9.72 J	11.76 J	21.0%

4.3 Performance comparison of HC, RHC and KHC

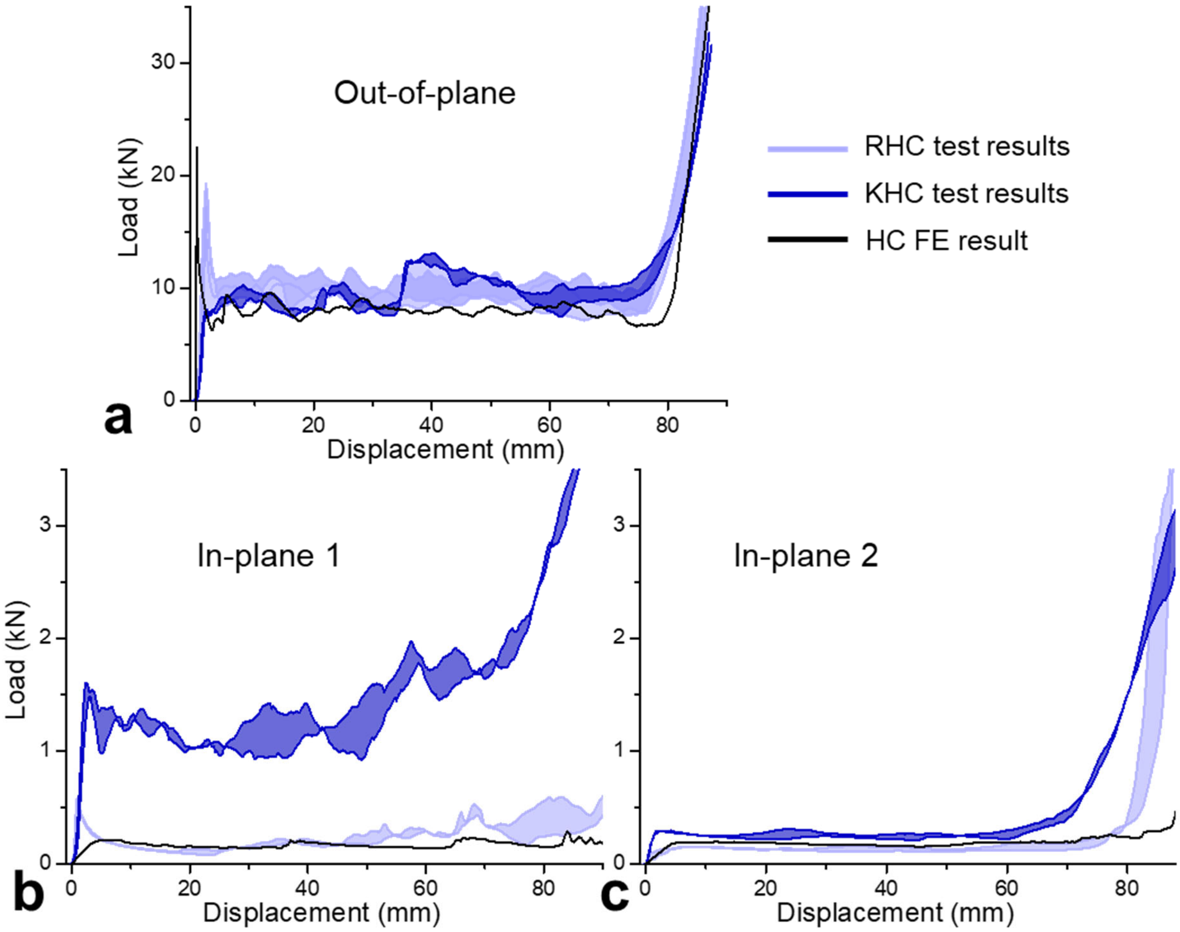

Figure 15. Load-displacement curves of three honeycombs under (a) out-of-plane; (b) in-plane 1; (c) in-plane 2 compression

The corrugation sheet thickness of HC is increased to 0.297 mm to achieve the relative density of 2.3%, same as the other two tested specimens. Comparisons of the load-displacement curves among RHC, KHC and the HC with adjusted wall thickness are shown in Figure 15, the load-displacement data of KHC and RHC are from the tests and are shaded in Figure 15 to cover the variations obtained in the test. Some key compressive parameters including initial peak, average crushing force and uniformity ratio of the three structures are listed Table 5, where these parameters of RHC and KHC were averaged from the test data. Compared to HC with 2% relative density, the initial peak force of FE result for HC with 2.3% relative density increases from 17.79 kN to 22.51kN. As previously studied [19], the critical load or the initial peak force of honeycomb structure under out-of-plane crushing is in a power relationship with the wall thickness, a slight increase (14% in this case from 0.26 to 0.297 mm) in wall thickness could lead to a large increase in initial peak force (27% increase in this case, from 17.79 kN to 22.51 kN). Therefore, to increase the energy absorption capacity of HC, alternatives should be considered rather than simply increase the wall thickness, as a significant increase in initial peak force could lead to severe damage to the protected structure.

Table 5. Comparisons of key compressive properties of HC with adjusted wall thickness, RHC and KHC under compression in three axial directions

	Out-of-plane			In-plane 1			In-plane 2		
	P_{peak}	P_{ave}	U	P_{peak}	P_{ave}	U	P_{peak}	P_{ave}	U
HC	22.51kN	8.06kN	2.79	213N	170N	1.25	196N	189N	1.04
RHC	18.05kN	9.63kN	1.87	517N	252N	2.05	156N	149N	1.05
KHC	9.67kN	9.48kN	1.02	1547N	1299N	1.19	282N	266N	1.06

A radar chart is shown in Figure 16, to illustrate the energy absorption capacity of the three honeycombs under compression in three axial directions. Compared to the HC, RHC still shows a superior energy absorption capacity under out-of-plane compression with a higher specific energy absorption as well as a more uniform crushing response. However, the advantage of RHC in terms of energy absorption under in-plane crushing is diminished. The in-plane 1 energy absorption of RHC is higher than that of HC, but it also introduces a high initial peak force. Under in-plane 2 crushing, RHC shows no advantage as compared to HC of the same density, with a low crushing resistance and a similar load-displacement response. Kirigami modified honeycomb (KHC) demonstrates superior energy absorption capacity over HC and RHC in all three axial directions. In out-of-plane compression, KHC exhibits excellent energy absorption with a higher crushing resistance than HC and a comparable average crushing resistance as RHC with nearly no initial peak force, owing to the unique fold-ins near the crushing interfaces. The crushing resistance of KHC along in-plane 1 direction is almost 7.5 times and 5.2 times than that of HC and RHC while maintaining a low initial peak force. Under in-plane 2 compression, KHC shows less enhancement in crushing resistance with a 40.7% and a 78.5% increase over HC and RHC, respectively. However, it should be noted that the second stage of deformation with a significant increase in crushing resistance occurs at around 70 mm of displacement for KHC under in-plane 2 compression as shown in Figure 15 (c). Since the 'densification' like sudden rise in crushing resistance is shown at around 70 mm, this second stage is therefore not included for calculating energy absorption of KHC along in-plane 2 direction, although the actual densification is not yet reached at 70 mm. Overall, in terms of energy absorption, RHC shows superiority over HC only under out-of-plane crushing, while KHC significantly outperforms both HC and RHC under out-of-plane and in-plane 1 compression, moderately outperforms HC and RHC under in-plane 2 compression.

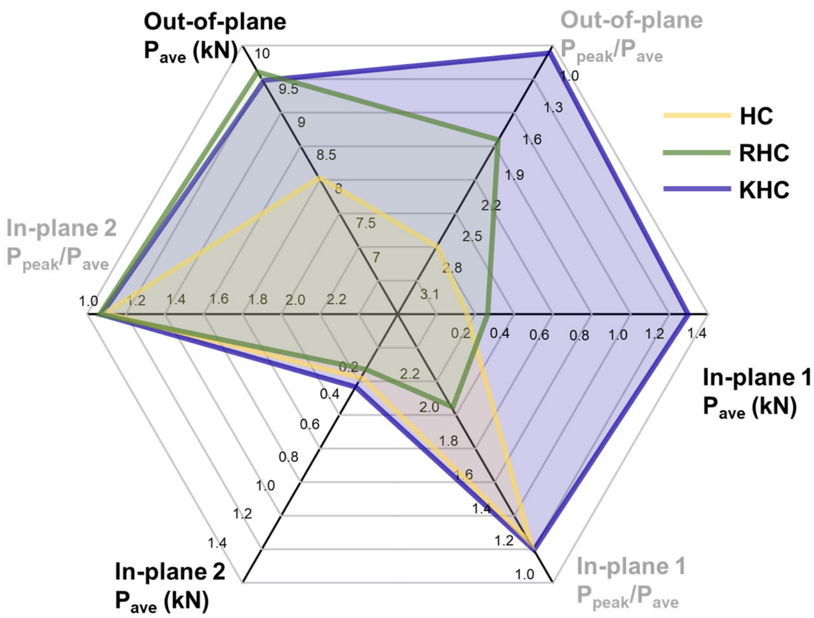

Figure 16. Comparison of average crushing resistance and uniformity ratio among HC, RHC and KHC under compression in three axial directions

5 Conclusion

Based on a Kirigami modification of a unit cell of corrugated structure, a new Kirigami modification on corrugation-manufactured honeycomb structure is proposed to enhance the energy absorption characteristics of standard honeycomb structure. Its compressive properties are investigated and compared with standard honeycomb and sheet reinforced honeycomb, which is one of the only commercially available modified honeycomb structure. Quasi-static crushing tests were carried out for these three honeycomb structures, including the standard honeycomb (HC), sheet reinforced honeycomb (RHC) and Kirigami modified honeycomb (KHC) under compression in three axial directions. To ensure a fair comparison among the structures, a numerical model of honeycomb structure was developed and validated with test data, and the wall thickness of HC numerical model was then adjusted so that all three honeycomb structures have the same relative densities. The main conclusions are given below.

1. The reinforced honeycomb (RHC) shows an improved energy absorption performance than standard honeycomb (HC) only under out-of-plane compression, with an increased average crushing resistance and a more uniform crushing. However, RHC shows similar or slightly worse energy absorption performance than HC under crushing in both in-plane directions.
2. Kirigami modified honeycomb (KHC) demonstrated significant improvement of energy absorption performance as compared to the other two honeycombs in all three axial directions, especially under out-of-plane and in-plane 1 crushing.
3. For crushing in the out-of-plane direction, KHC does not develop an initial peak force due to its unique fold-ins near two contacting interfaces, while its average crushing resistance remains at a similar level as RHC, higher than that of HC.
4. For the in-plane 1 compression, the average crushing resistance of KHC is around 5.2 and 7.5 times of that of HC and RHC, with an even lower uniformity ratio.
5. KHC shows a moderate improvement in crushing resistance in in-plane 2 direction, compared with the other two honeycombs.

Overall, KHC shows a significant enhancement in energy absorption characteristic of honeycomb structure in three axial directions, with minimal altering on its corrugation manufacturing process.

Acknowledgements

The financial support from the Australian Research Council via Discovery Early Career Researcher Award (DE160101116) is acknowledged.

Reference

[1] K.F. Karlsson, B. TomasÅström, Manufacturing and applications of structural sandwich components, Composites Part A: Applied Science and Manufacturing, 28 (1997) 97-111.

[2] X. Yang, J. Ma, D. Wen, J. Yang, Crashworthy design and energy absorption mechanisms for helicopter structures: A systematic literature review, Progress in Aerospace Sciences, 114 (2020).

[3] A.S. Herrmann, P.C. Zahlen, I. Zuardy, Sandwich structures technology in commercial aviation, in: Sandwich structures 7: Advancing with sandwich structures and materials, Springer, 2005, pp. 13-26.

[4] R. Chatys, A. Panich, R.S. Jurecki, M. Kleinhofs, Composite materials having a layer structure of "sandwich" construction as above used in car safety bumpers, in: Automotive Safety, 2018 XI International Science-Technical Conference, IEEE, 2018, pp. 1-8.

[5] Z. Wang, J. Liu, Z. Lu, D. Hui, Mechanical behavior of composited structure filled with tandem honeycombs, Composites Part B: Engineering, 114 (2017) 128-138.

[6] T. Wierzbicki, Crushing analysis of metal honeycombs, International Journal of Impact Engineering, 1 (1983) 157-174.

[7] T. Wierzbicki, W. Abramowicz, On the crushing mechanics of thin-walled structures, Journal of Applied mechanics, 50 (1983) 727-734.

[8] W. Abramowicz, T. Wierzbicki, Axial Crushing of Multicorner Sheet Metal Columns, Journal of Applied Mechanics, 56 (1989) 113-120.

[9] F. Côté, V.S. Deshpande, N.A. Fleck, A.G. Evans, The out-of-plane compressive behavior of metallic honeycombs, Materials Science and Engineering: A, 380 (2004) 272-280.

[10] D.D. Radford, G.J. McShane, V.S. Deshpande, N.A. Fleck, Dynamic Compressive Response of Stainless-Steel Square Honeycombs, Journal of Applied Mechanics, 74 (2007) 658.

[11] K.P. Dharmasena, H.N.G. Wadley, Z. Xue, J.W. Hutchinson, Mechanical response of metallic honeycomb sandwich panel structures to high-intensity dynamic loading, International Journal of Impact Engineering, 35 (2008) 1063-1074.

[12] F. Zhu, L. Zhao, G. Lu, Z. Wang, Deformation and failure of blast-loaded metallic sandwich panels—Experimental investigations, International Journal of Impact Engineering, 35 (2008) 937-951.

[13] G.N. Nurick, G.S. Langdon, Y. Chi, N. Jacob, Behaviour of sandwich panels subjected to intense air blast – Part 1: Experiments, Composite Structures, 91 (2009) 433-441.

[14] S. Deqiang, Z. Weihong, W. Yanbin, Mean out-of-plane dynamic plateau stresses of hexagonal honeycomb cores under impact loadings, Composite Structures, 92 (2010) 2609-2621.

[15] S. Xu, J.H. Beynon, D. Ruan, G. Lu, Experimental study of the out-of-plane dynamic compression of hexagonal honeycombs, Composite Structures, 94 (2012) 2326-2336.

[16] Z. Wang, H. Tian, Z. Lu, W. Zhou, High-speed axial impact of aluminum honeycomb – Experiments and simulations, Composites Part B: Engineering, 56 (2014) 1-8.

[17] L.J. Gibson, M.F. Ashby, Cellular solids: structure and properties, Cambridge university press, 1999.

[18] L.L. Hu, T.X. Yu, Dynamic crushing strength of hexagonal honeycombs, International Journal of Impact Engineering, 37 (2010) 467-474.

[19] J. Zhang, M. Ashby, The out-of-plane properties of honeycombs, International Journal of Mechanical Sciences, 34 (1992) 475-489.

[20] G. Lu, T. Yu, Energy Absorption of Structures and Materials, Woodhead publishing limited, Cambridge England, 2003.

[21] Z. Li, W. Chen, H. Hao, Blast mitigation performance of cladding using Square Dome-shape Kirigami folded structure as core, International Journal of Mechanical Sciences, 145 (2018) 83-95.

[22] H.N. Wadley, Multifunctional periodic cellular metals, Philos Trans A Math Phys Eng Sci, 364 (2006) 31-68.

[23] Hexcel®Corporation, HexWeb® Honeycomb: Attributes and Properties-A comprehensive guide to standard Hexcel honeycomb materials, configurations, and mechanical properties., in, 2019.

[24] A. Alantali, R.A. Alia, R. Umer, W.J. Cantwell, Energy absorption in aluminium honeycomb cores reinforced with carbon fibre reinforced plastic tubes, Journal of Sandwich Structures & Materials, (2017) 109963621772714.

[25] Z. Wang, J. Liu, Mechanical performance of honeycomb filled with circular CFRP tubes, Composites Part B: Engineering, 135 (2018) 232-241.

[26] Y. Zhang, L. Yan, W. Zhang, P. Su, B. Han, S. Guo, Metallic tube-reinforced aluminum honeycombs: Compressive and bending performances, Composites Part B: Engineering, 171 (2019) 192-203.

[27] Y. Zhang, L. Yan, C. Zhang, S. Guo, Low-velocity impact response of tube-reinforced honeycomb sandwich structure, Thin-Walled Structures, 158 (2021).

[28] B. Han, K. Qin, B. Yu, B. Wang, Q. Zhang, T.J. Lu, Honeycomb–corrugation hybrid as a novel sandwich core for significantly enhanced compressive performance, Materials & Design, 93 (2016) 271-282.

[29] G. Sun, S. Li, Q. Liu, G. Li, Q. Li, Experimental study on crashworthiness of empty/aluminum foam/honeycomb-filled CFRP tubes, Composite Structures, 152 (2016) 969-993.

[30] N.A.Z. Abdullah, M.S.M. Sani, M.S. Salwani, N.A. Husain, A review on crashworthiness studies of crash box structure, Thin-Walled Structures, 153 (2020).

[31] Y. Cheng, M. Liu, P. Zhang, W. Xiao, C. Zhang, J. Liu, H. Hou, The effects of foam filling on the dynamic response of metallic corrugated core sandwich panel under air blast loading – Experimental investigations, International Journal of Mechanical Sciences, (2018).

[32] H. Mozafari, S. Khatami, H. Molatefi, V. Crupi, G. Epasto, E. Guglielmino, Finite element analysis of foam-filled honeycomb structures under impact loading and crashworthiness design, International Journal of Crashworthiness, 21 (2016) 148-160.

[33] D. Pietras, E. Linul, T. Sadowski, A. Rusinek, Out-of-plane crushing response of aluminum honeycombs in-situ filled with graphene-reinforced polyurethane foam, Composite Structures, 249 (2020).

[34] Y. Zhang, Q. Liu, Z. He, Z. Zong, J. Fang, Dynamic impact response of aluminum honeycombs filled with Expanded Polypropylene foam, Composites Part B: Engineering, 156 (2019) 17-27.

[35] Q. He, D.W. Ma, Parametric study and multi-objective crashworthiness optimisation of reinforced hexagonal honeycomb under dynamic loadings, International Journal of Crashworthiness, 20 (2015) 495-509.

[36] G. Tiwari, T. Thomas, R.P. Khandelwal, Influence of reinforcement in the honeycomb structures under axial compressive load, Thin-Walled Structures, 126 (2018) 238-245.

[37] J. Zhang, G. Lu, D. Ruan, X. Huang, Experimental observations of the double shock deformation mode in density graded honeycombs, International Journal of Impact Engineering, 134 (2019) 103386.

[38] Z. Zhang, H. Lei, M. Xu, J. Hua, C. Li, D. Fang, Out-of-plane compressive performance and energy absorption of multi-layer graded sinusoidal corrugated sandwich panels, Materials & Design, 178 (2019).

[39] G.W. Kooistra, V. Deshpande, H.N. Wadley, Hierarchical corrugated core sandwich panel concepts, Journal of applied mechanics, 74 (2007) 259-268.

[40] Y. Zhang, M. Lu, C.H. Wang, G. Sun, G. Li, Out-of-plane crashworthiness of bio-inspired self-similar regular hierarchical honeycombs, Composite Structures, 144 (2016) 1-13.

[41] S. Li, Z. Liu, V.P.W. Shim, Y. Guo, Z. Sun, X. Li, Z. Wang, In-plane compression of 3D-printed self-similar hierarchical honeycombs – Static and dynamic analysis, Thin-Walled Structures, 157 (2020).

[42] S. Townsend, R. Adams, M. Robinson, B. Hanna, P. Theobald, 3D printed origami honeycombs with tailored out-of-plane energy absorption behavior, Materials & Design, 195 (2020).

[43] Z. Li, Q. Yang, R. Fang, W. Chen, H. Hao, Origami metamaterial with two-stage programmable compressive strength under quasi-static loading, International Journal of Mechanical Sciences, 189 (2021).

[44] Hexcel®Corporation, HexWeb® Rigicell™ Corrosion Resistant Aluminum Corrugated Honeycomb Product Data, in, 2014.

[45] Z. Li, W. Chen, H. Hao, Q. Yang, R. Fang, Energy absorption of kirigami modified corrugated structure, Thin-Walled Structures, 154 (2020) 106829.

[46] ASTM, E8M-04 Standard Test Methods for Tension Testing of Metallic Materials (Metric) 1, ASTM international, 2004.

[47] A. Sadighi, A. Eyvazian, M. Asgari, A.M. Hamouda, A novel axially half corrugated thin-walled tube for energy absorption under Axial loading, Thin-Walled Structures, 145 (2019).

[48] R.K. Fathers, J.M. Gattas, Z. You, Quasi-static crushing of eggbox, cube, and modified cube foldcore sandwich structures, International Journal of Mechanical Sciences, 101-102 (2015) 421-428.